ACS Energy LETTERS

http://pubs.acs.org/journal/aelccp

Metal Nitride as a Mediator for the Electrochemical Synthesis of NH_3

Ishita Goyal,[#] Nishithan C. Kani,[#] Samuel A. Olusegun, Sreenivasulu Chinnabattigalla, Rajan R. Bhawnani, Ksenija D. Glusac, Aayush R. Singh,* Joseph A. Gauthier,* and Meenesh R. Singh*

Cite This: *ACS Energy Lett.* 2024, 9, 4188−4195

Read Online

ACCESS | Metrics & More | Article Recommendations | Supporting Information

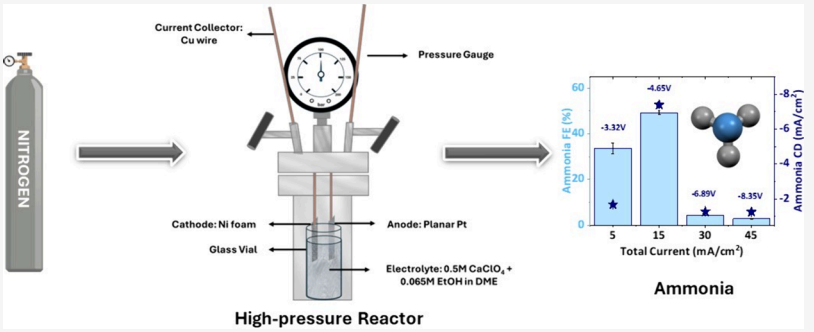

ABSTRACT: **The Haber-Bosch process has a massive carbon footprint, and it is highly desired to decentralize NH_3 synthesis in a more sustainable manner. Li-mediated NH_3 electrosynthesis is a promising approach to making NH_3 under ambient conditions, but it suffers from poor energy efficiency owing to the highly reducing electroplating potential of Li. In this Letter, we report a combined theoretical and experimental investigation into other mediators beyond Li, such as Ca, Mg, Sr, Y, and V. The density functional theory results suggest that, besides Li, Ca and Mg can also activate N_2 at room temperature and have a stable surface nitride vacancy necessary for NH_3 synthesis. NH_3 faradaic efficiencies of 50% ± 0.2% and 27% ± 2% are obtained from Ca and Mg, respectively, at an applied current density of 15 mA/cm^2. This Letter serves as a proof-of-concept for Li-free NH_3 synthesis and will motivate further research in metal-nitride-mediated processes.**

Mitigating climate change is one of the biggest challenges of this century. NH_3 synthesis by the Haber-Bosch process contributes to 1% to 2% of the total greenhouse gas emissions,[1,2] largely because the process is exceptionally energy-intensive, requiring extreme temperatures (>700 K) and pressures (>100 atm).[1−5] Decarbonizing NH_3 synthesis has therefore attracted considerable attention, with an electrochemical synthesis route possibly enabling carbon-free, decentralized NH_3 production using renewable energy. Previous efforts to directly synthesize NH_3 electrochemically from N_2 and H_2O at ambient conditions have struggled to overcome the competing H_2 evolution reaction (HER).[4] An efficient electrocatalyst to synthesize NH_3 by selectively reducing N_2 instead of H_2O has yet to be discovered. The electrochemical NH_3 synthesis in aqueous medium suffers from low NH_3 Faradaic efficiencies (FE) and current densities and requires a breakthrough.[6,7] Due to low NH_3 yields, several reports are not reproducible,[8] and a rigorous protocol to perform the direct electrochemical N_2 reduction has been developed in the literature.[9]

In contrast, considerable progress has been made in the past five years toward the Li-mediated NH_3 synthesis (Li-MAS) process.[10−12,7,12−23] However, fundamental aspects of the process remain poorly understood, such as the mechanism of NH_3 synthesis, formation of the solid-electrolyte interface (SEI), and transport across it.[24,15] Here, we hypothesize a mechanism illustrated in Scheme 1, which involves the following steps: (1) electrodeposition of Li onto the metallic substrate (e.g., Ni, Cu); (2) spontaneous reaction of Li metal with N_2 to form Li_3N; (3) protonation of Li_3N with a proton donor (e.g., ethanol) to form NH_3 and a *surface* N vacancy on the lithium nitride; (4) exergonic binding of N_2 in the N vacancy site on lithium nitride; (5) reduction of N_2 via an

Received: May 29, 2024
Revised: July 12, 2024
Accepted: July 24, 2024

https://doi.org/10.1021/acsenergylett.4c01455
ACS Energy Lett. 2024, 9, 4188−4195

Scheme 1. Schematic Overview of Metal-Nitride Mediated Ammonia Synthesis[a]

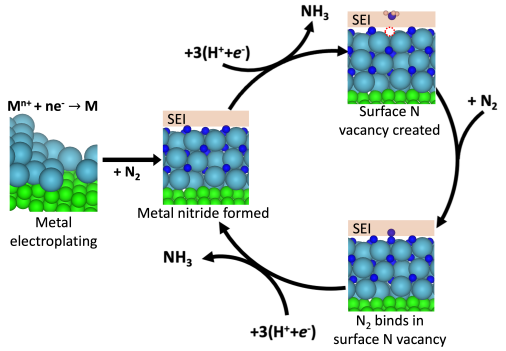

[a]In addition to the above process, competition from undesired hydrogen evolution reaction (HER) may occur via coupled proton−electron transfer (CPET) steps either on the metal nitride surface or in the surface N vacancy.

associative mechanism,[25] recovering lithium nitride and closing the catalytic cycle. Note that this hypothesized mechanism does not involve concomitant corrosion of Li into solution, which should be endergonic at the applied potentials typically used.[13]

Previous studies have illustrated that a maximum NH_3 FE of ∼100% and NH_3 current density of ∼−700 mA/cm^2 can be obtained by using imide-based Li salts.[7] A continuous flow NH_3 synthesis has been developed by Fu et al. by utilizing H_2 oxidation on the Pt−Au alloy anode with 61% NH_3 FE.[20] The Li-mediated NH_3 synthesis process suffers from low energy efficiency (well below that of the legacy Haber-Bosch process) due to the need for extremely reducing plating potential of Li (∼−3.04 V vs SHE). As such, identifying an alternative mediator for this process with a less reducing electroplating potential is highly desired. Tort et al.[26] developed a systematic approach to investigate catalytic systems for the electrochemical fixation of N_2, specifically focusing on understanding the unique role of Li as a mediator in electrochemical NH_3 synthesis. In their experimental investigations, other mediators such as Ca and Mg were inactive for electrochemical N_2 activation at reported experimental conditions.

Given the hypothesized mechanism above, several criteria for a successful mediator of NH_3 electrosynthesis must be met simultaneously and have been identified previously[27] including:

(1) spontaneous formation of a nitride in the presence of N_2, (i.e., thermodynamics) and facile activation of N_2 on the metal (i.e., kinetics)
(2) stability of a *surface* N vacancy in the nitride with respect to the *bulk* nitride
(3) exergonic binding of N_2 at a surface N vacancy of the nitride
(4) solubility of salts of the mediator in nonaqueous electrolyte
(5) facile diffusion of N in the bulk nitride

Here, we argue that the final criteria (5), facile diffusion of N in the bulk nitride, is not necessary: although a *surface* nitride must form, only a few layers are necessary to achieve the desired effect given the "near-sightedness" of metals with respect to distant perturbations.[28−30]

In addition to our first report on calcium-mediated ammonia synthesis (Ca-MAS),[31] a following report from Fu et al.[32] demonstrated Ca-mediated NH_3 synthesis in a flow system and achieved 40 ± 2% NH_3 FE at −2 mA/cm^2 by using $Ca[B(hfip)_4]_2$ as the electrolyte. Here, we are able to demonstrate Ca mediated NH_3 synthesis by using calcium perchlorate salt in dimethyl ether, achieving 50 ± 0.2% NH_3 FE at an applied current density of −15 mA/cm^2 and 6 bar N_2 pressure.

Figure 1A shows a theoretical descriptor for criteria (2), surface nitride vacancy stability, and (3), facile activation of N_2

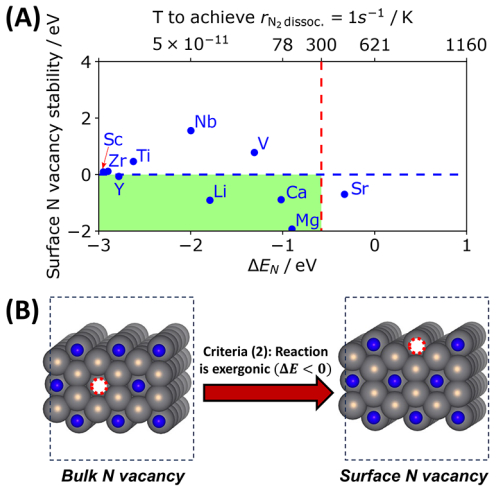

Figure 1. (A) Selected theoretical criteria for a successful mediator of electrochemical NH_3 synthesis, adapted with permission from ref 27. Criteria include the stability of a surface N vacancy with respect to the bulk nitride and the spontaneous formation of a surface nitride under ambient conditions. The temperature to achieve N_2 dissociation turnover frequency of 1 s^{-1} was calculated by assuming a transition metal Brønsted−Evans−Polanyi (BEP) scaling from ref 34. The vertical dashed line represents N_2 dissociation at room temperature. Here, we identify both Ca and Mg as feasible mediators for the process in addition to Li. (B) Schematic illustration of criteria (2), quantitatively illustrated as the *y*-axis of (A).

at a surface vacancy of the nitride in the SEI. The *y*-axis of Figure 1A corresponds to the energy required to move a bulk vacancy to the surface (or, equivalently, the energy required to move a surface N to fill a bulk vacancy); i.e., following the approach of Nørskov and Cargnello,[33] the energy of the surface vacancy relative to the bulk is the difference between the free energies of vacancy on surface nitride and the vacancy inside the bulk nitride, which is illustrated in Figure 1B,

$$\Delta E^{\mathrm{vac}}_{\mathrm{surf}\rightarrow\mathrm{bulk}} = E^{\mathrm{vac}}_{\mathrm{surf}} - E^{\mathrm{vac}}_{\mathrm{bulk}} \quad (1)$$

If this quantity is positive, a thermodynamic driving force would exist for the continuous transition of surface N vacancies to the bulk, inhibiting the adsorption of N_2 at the surface N vacancy site. As such, a successful mediator of this process should exhibit surface N vacancies that are stable with respect to the bulk, i.e., $\Delta E^{\mathrm{vac}}_{\mathrm{surf}\rightarrow\mathrm{bulk}} < 0$. Note that this criteria is consistent with discarding facile bulk N diffusion as a necessary criteria for a mediator: formation of a *bulk* nitride (i.e., more than 3−5 monolayers of nitride) is not necessary, since a material with stable surface N vacancies will not electronically interact with the bulk nitride due to the aforementioned near-

https://doi.org/10.1021/acsenergylett.4c01455
ACS Energy Lett. 2024, 9, 4188−4195

sightedness of metals.[28−30] We further note that, in reactors with significantly improved transport of N_2, this criteria may be unnecessary, as NH_3 could be displaced by N_2 without forming the surface N vacancy.

Figure 1A also addresses criterion (1), facile activation of N_2 as the two *x*-axes. The clean metal (i.e., before nitride formation) must bind N strongly enough to rapidly dissociate N_2, ideally under ambient conditions. To address this, we assume a Brønsted−Evans−Polanyi (BEP) scaling found in transition metals[34] to map the calculated ΔE_N values to activation barriers for N_2 dissociation. It assumes a linear free energy relationship between the driving force and the reaction barrier. We verified this approximation by calculating the N_2 activation barrier on Ca (211) using DFT and found the process to be barrierless, with a significantly exergonic reaction energy ($2\Delta E_N = -2.6$ eV) as suggested by the reported ΔE_N in Figure 1A. Here, we find $E_{A,\,N_2\,dissoc.} \approx 1.56\Delta E_N + 1.38$, in units of eV. To determine the upper *x*-axis of Figure 1A, we solve the following nonlinear rate equation for T,

$$r_{N_2 dissoc.} = 1 s^{-1} = \frac{k_B T}{h} {p_{N_2}}^{0.5} \theta_* \exp\left[-\frac{\Delta G_{A,N_2 dissoc.}}{k_B T}\right] \quad (2)$$

Here, k_B and h are the Boltzmann and Planck constants, p_{N_2} is the nitrogen pressure (taken to be 1 bar), θ_* is the coverage of free sites on the surface (approximated as 1), and $\Delta G_{A,\,N_2\,dissoc.}$ is the Gibbs free energy of N_2 activation. For T = 300 K, we calculate a corresponding ΔE_N of approximately −0.6 eV, forming the vertical red line in Figure 1A and enclosing the green box, which denotes viable candidates as mediators for this process. Note that all materials in Figure 1A satisfy criteria (1) from the thermodynamics perspective (i.e., they all spontaneously form nitrides in the presence of N_2). Here, the vertical line illustrates those that our DFT calculations suggest will form a *surface* nitride at room temperature. Note also that our analysis neglects criteria (5), the existence of salts soluble in nonaqueous electrolytes.

Here, we wish to highlight that the system being investigated here−metal/metal nitrides in contact with a nonaqueous electrolyte under highly reducing conditions−is exceptionally complex, and so verifying our hypothesized mechanism conclusively is, at present, not possible. A study by Tort et al.,[26] which proposes a different mechanism, yet arrives at a similar list of possible mediators of this process, further highlighting the complexity. Experimental control studies testing some of the criteria outlined above would be useful areas of future research. For example, an experiment in which the cathode begins as a nitride material and with no salt in solution may test the hypothesis that surface N vacancies in the nitride are the key active site for this process.

Among the identified mediators beyond Li, we explored Ca and Mg experimentally as candidates for N_2 activation and electrochemical NH_3 synthesis. Ca was chosen for detailed analysis because it is predicted to be the most reactive (i.e., Ca binds N stronger than Mg), and it has a standard reduction potential of Ca (−2.87 V vs SHE) close to Li (−3.04 V vs SHE), suggesting that a similar experimental protocol may succeed. The formation of Ca_3N_2 is favorable due to the spontaneous reaction of N_2 and Ca, as the free energy of the formation of Ca_3N_2 is −4 eV. It is known that the formation of a bulk nitride can be kinetically slow,[35,36] but as discussed above, we hypothesize that bulk nitride formation is not necessary for a successful mediator of this process. We hypothesize that Ca-MAS occurs in a process analogous to Li-MAS, i.e., based on the following reaction scheme and also shown in Scheme 1:

[**Ca electrodeposition**]

$$Ca^{2+} + 2e^- \rightarrow Ca_{(s)} \quad (i)$$

[**Ca nitridation**]

$$6Ca_{(s)} + N_{2(aq)} \rightarrow 2Ca_3N_{2(s)} \quad (ii)$$

[**Ca_3N_3 protolysis**]

$$Ca_3N_{2(s)} + HX + e^- \rightarrow Ca_3N{-}NH \quad (iii)$$

[**Ca_3N_2H protolysis**]

$$Ca_3N{-}NH^* + HX + e^- \rightarrow Ca_3N{-}NH_2 + X^- \quad (iv)$$

[**$Ca_3N_2H_2$ protolysis**]

$$Ca_3N{-}NH_2 + HX + e^- \rightarrow Ca_3N{-}NH_3 + X^- \quad (v)$$

NH_3 desorption

$$Ca_3N{-}NH_3 \rightarrow Ca_3N^* + NH_{3(aq)} \quad (vi)$$

[**Ca_3N^* nitridation**]

$$Ca_3N^* + \frac{1}{2}N_2 \rightarrow Ca_3N_{2(s)} \quad (vii)$$

First, Ca is electrodeposited on a substrate by dissolving Ca salt in a nonaqueous solvent (Calcium Electrodeposition, eq i) and applying a strongly reducing bias on the cathode. The electrodeposited Ca metal reacts spontaneously with N_2 (either dissolved or gaseous in a GDE setup) to form Ca_3N_2 (Calcium Nitridation, eq ii). Following the formation of Ca_3N_2, a sequence of coupled proton-electron transfer (CPET) steps (eqs iii−v) forms NH_3 adsorbed to calcium nitride (Calcium Nitride Protolysis). Finally, NH_3 desorbs, forming a surface N vacancy on the calcium nitride (eq vi). Given the stability of this surface nitride vacancy shown in Figure 1A,[36] we hypothesize that it is filled by N_2, which is subsequently reduced by an associated mechanism in a sequence of CPET reactions, thereby completing the catalytic cycle. Ca metal and nitride can also serve as catalysts for hydrogen evolution to form H_2, an undesired side reaction (Calcium Protolysis). We again note that this proposed mechanism is slightly different than those appearing in some published reports for the analogous Li-MAS process,[13,15] which has been hypothesized to involve the concomitant dissolution of Li to form Li^+. As discussed above, the precise mechanism is still poorly understood and likely depends strongly on specific details of the experimental protocol in use (e.g., dynamic potential control, electrolyte and salt choice, N_2 pressure, and others). However, we hypothesize here that concomitant dissolution cannot occur under the strongly reducing conditions typically used, as the corrosion subreaction will be endergonic. In this Letter, we provide a proof of concept for the Ca and Mg-mediated NH_3 synthesis.

From our prior work and literature reports on Li-MAS, we observe that increased N_2 pressure results in improved NH_3

https://doi.org/10.1021/acsenergylett.4c01455
ACS Energy Lett. 2024, 9, 4188−4195

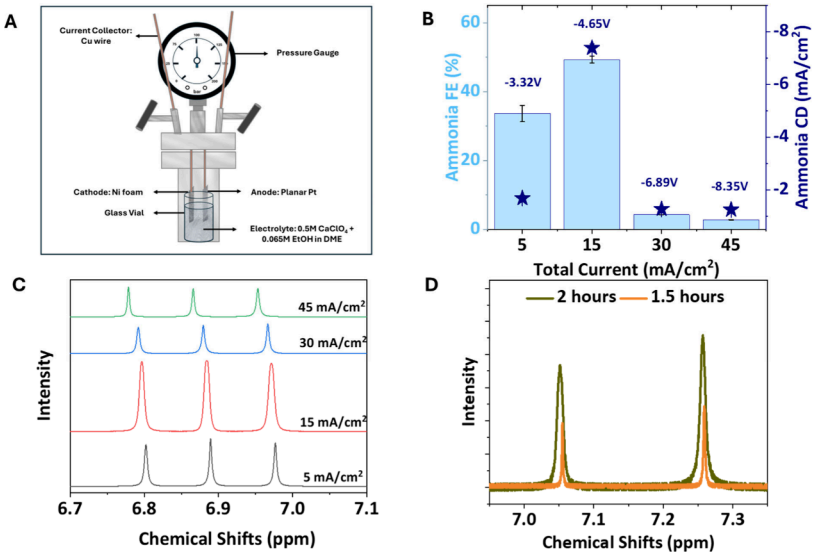

Figure 2. (A) Schematic and configuration of the batch autoclave for electrochemical ammonia synthesis. (B) NH_3 FE and NH_3 current density (CD) at different applied CDs. (C) ^1H NMR spectra for ^{14}N experiments at varying current densities. (D) ^1H NMR spectra for ^{15}N experiment at −15 mA/cm^2.

FE.[10,13] This enhancement extends only to a certain level beyond which there is no improvement in the NH_3 FE as the system is no longer in an N_2 mass transport limited regime.[10] Similarly, there exists an optimal concentration of the proton donor which balances the Li_3N protolysis (toward NH_3) and Li protolysis (toward HER) steps. Hence, for Ca-MAS, we operate our reactor at a slightly elevated N_2 pressure of 6 bar. Ethanol (EtOH, also referred to as HX in eqs iii, iv, and v) was used as the proton donor at a concentration of 0.65 M. The reaction was carried out in a modified autoclave setup to withstand high pressures, as shown in Figure 2A. Ni foam was used as the cathode; Pt was used as the anode in a membraneless setup, and the electrolyte was stirred at 700 rpm. Tetrahydrofuran (THF) is commonly used as an aprotic solvent to dissolve Li salts in Li-MAS. One of the challenges inCa-MAS is to have a suitable Ca salt that can be dissolved in an aprotic solvent. Calcium salts generally have poor solubility in water and are mostly insoluble in nonaqueous solvents. The Ca salts that are soluble in water generally exist in their hydrated form, as they are hygroscopic. Among the tested Ca salts, $Ca(ClO_4)_2$ has good solubility in dimethyl ether (DME). The water content in freshly prepared preelectrolytes was measured using a Karl Fischer titrator, yielding an average value of 3.04 ± 0.12%. Experiments were conducted at varying current densities, ranging from 5 mA/cm^2 up to 45 mA/cm^2, as illustrated in Figure 2B. At lower current densities, calcium deposition rate is lower, resulting in a decrease in available Ca sites for nitridation steps, leading to lesser formation of calcium surface nitride. As the current density and, hence, the cell potential increases, the selectivity of calcium nitride protolysis vs calcium protolysis seems to improve, as interpreted from the increased FE of NH_3 in Figure 2B. At −15 mA/cm^2, the calcium nitridation and calcium nitride protolysis steps seems to reach an optimal balance, resulting in the maximum NH_3 FE of 50%. At higher current densities, such as −30 mA/cm^2 and −45 mA/cm^2, the cell voltage rapidly increases as denoted in Figure S2A which could lead to electrochemical degradation of the solvent and poor formation of the SEI. Hence, we observe a low NH_3 FE at higher current densities. An optimal cell voltage of ∼4 V is required for stable performance.

Quantitative analysis of ammonia was conducted using ^1H NMR spectroscopy, following the previously published protocol that ensures that the measured NH_3 arises from the electrochemical N_2 reduction and not from air or other potential contamination sources.[9] The approach involves the use of the $^{15}N_2$ isotope as a substrate for electrochemical N_2 reduction. Since the ^{15}N isotope is a spin 1/2 nucleus, the ^1H NMR spectrum of the ammonia electrogenerated from $^{15}N_2$ will give a characteristic doublet at 7.52 ppm with a coupling constant of 180 Hz. This doublet can be readily distinguished from the triplet peak associated with ammonia containing the most abundant ^{14}N isotope (spin 1 nucleus), which appears at 6.89 ppm with a coupling constant of 54 Hz. The resulting spectra for the post-electrolyte samples at different current densities are depicted in Figure 2C. Isotope labeling experiments were conducted at −15 mA/cm^2, as this condition yielded the highest FE and ammonia current density. The isotope-labeled experiments were quantified by using ^1H NMR, as depicted in Figure 2D, resulting in an FE of 50 ± 0.2% at −15 mA/cm^2. Rigorous control experiments were performed to ensure that NH_3 is produced by the electrochemical reduction of N_2 and not from adverse contaminants (see Supporting Information). To depict the accumulation of ammonia over time, two different experiments were performed in a batch system. One experiment ran for 2 h at −15 mA/cm^2, while the other ran for 1.5 h at −15 mA/cm^2. The isotope-labeled experiments were quantified using ^1H NMR, as depicted in Figure 2D, resulting in an FE of 50 ± 0.2% at −15 mA/cm^2. In the isotope labeling experiment conducted for 1.5 h at −15 mA/cm^2, an NH_3 FE of 38% was obtained, with an ammonia current density of 5.6 mA/cm^2. Open circuit control experiments were performed for both $^{14}N_2$ and $^{15}N_2$, where no potential was applied, and the solutions were kept on a stir plate for 2 h. NMR spectra of the pre-electrolyte and post-electrolyte samples for both cases showed no ammonia in the post-electrolyte samples, as shown in Figure S3A. Additionally, another control experiment was conducted

https://doi.org/10.1021/acsenergylett.4c01455
ACS Energy Lett. 2024, 9, 4188−4195

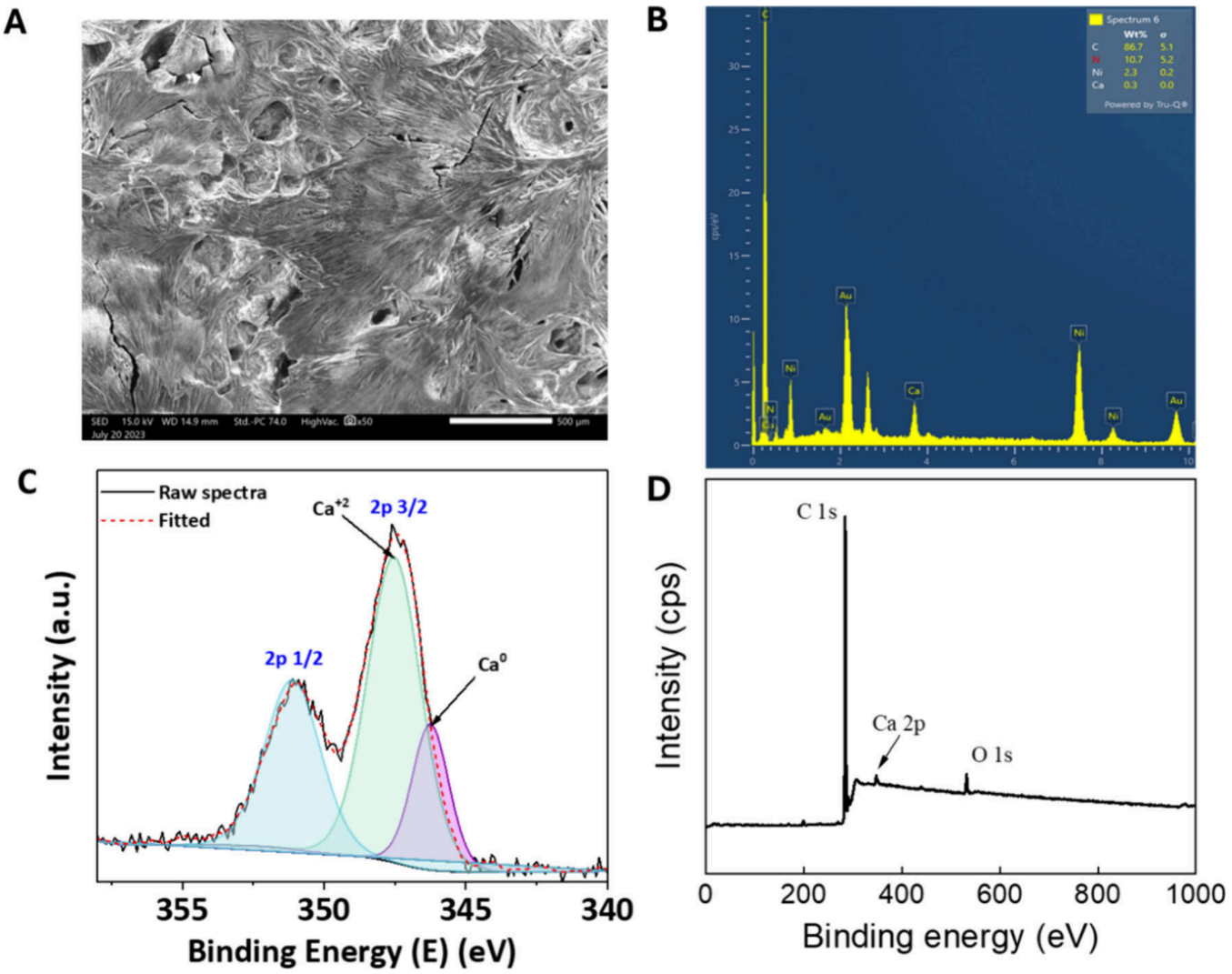

Figure 3. (A) SEM image of Ca deposited Ni foam post-electrolysis. (B) EDS spectrum of post-electrolyte electrode showing the presence of Ca and Ni. (C) High resolution XPS scan of the post-electrolysis electrode confirming the presence of Ca. (D) XPS survey scan of the post-electrolysis electrode showing the presence of O from perchlorate species.

using argon (Ar) to pressurize the reactor instead of N_2. The reactor was pressurized to 6 bar with Ar, and the reaction was carried out at -15 mA/cm^2 for 2 h. Post-electrolyte analysis using ^{1}H NMR showed no ammonia peaks as shown in Figure S3B. Finally, an electrolyte sample was prepared and left open in the fume hood to ensure that ammonia was not coming from atmospheric contaminants but was instead being electrochemically synthesized. After 2 h in the fume hood, ^{1}H NMR analysis showed no ammonia peaks as depicted in Figure S3B.

The characterization of the post-electrolysis catalyst was conducted using Scanning Electron Microscopy with Energy Dispersive X-ray Spectroscopy (SEM-EDS) and X-ray Photoelectron Spectroscopy (XPS) on the postreaction sample, as depicted in Figure 3. The analysis was performed ex situ just to confirm the deposition of Ca. In situ analysis to understand the interface would be interesting, but it is beyond the scope of the current work.

After establishing calcium as a successful mediator, we briefly investigated the potential of magnesium (Mg) as an alternative mediator. Similar experimental setups as employed in Ca-MAS were utilized for this study. One M magnesium perchlorate in N,N-dimethylformamide (DMF) with 0.065 M ethanol was used as the electrolyte. Chronopotentiometry was performed at a constant current density of 15 mA/cm^2. Detailed experimental methods are provided in the Supporting Information. Ammonia quantification was conducted using a UV−vis spectrometer and the indophenol method. To ensure accurate concentration estimation, the method of additions was followed as shown in Figure 4B. According to UV−vis quantifications, we obtained a Faradaic Efficiency (FE) of 27.2% ± 2.4% for Mg-mediated Ammonia Synthesis (Mg-MAS) with an ammonia current of -4.08 ± 0.26 mA/cm^2. Our observations were quantitatively validated using Nuclear Magnetic Resonance (^{1}H NMR) as depicted in Figure 4 which predicted 27.14% and 4.07 mA/cm^2 ammonia current density. The signature triplet for ammonia appears at 6.83 ppm in NMR with a coupling constant of 96 Hz. The operating cell voltage for magnesium was observed to be lower than that for calcium, which is consistent with DFT calculations. Detailed research on MgMAS is still ongoing; a comprehensive study is planned for future investigation.

The work presented in this paper demonstrates the Ca-mediated NH_3 synthesis and is one of the first few reported

https://doi.org/10.1021/acsenergylett.4c01455
ACS Energy Lett. 2024, 9, 4188−4195

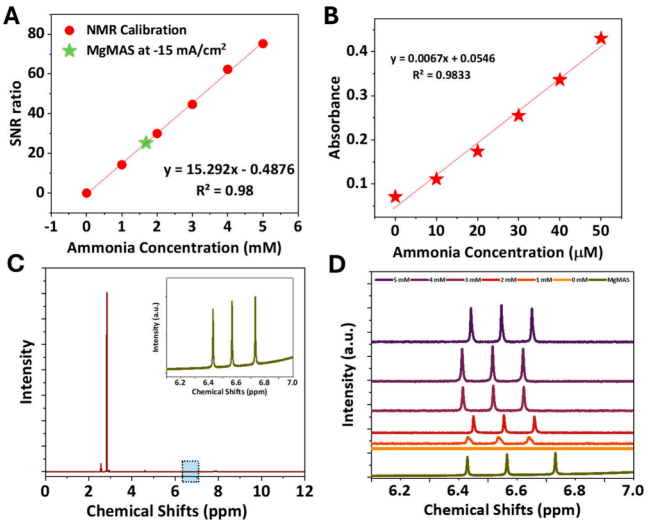

Figure 4. (A) $^{14}NH_3$ NMR calibration curve with a −15 mA/cm^2 data point for MgMAS. (B) UV−vis absorbances as a function of NH_3 concentrations at 632 nm for Mg-MAS post-electrolyte. (C) ^{1}H NMR spectra of Mg-MAS post-electrolyte at −15 mA/cm^2 with a cell voltage of −3.43 V. (D) NMR spectra of calibration of N-14 ammonia solution for MgMAS.

works in this domain. A maximum NH_3 FE of 50 ± 0.2% was obtained at −15 mA/cm^2. The process suffers from several challenges that must be overcome. Calcium salts are insoluble in most of the solvents explored here. Future studies screening the solubility of different Ca salts in different aprotic solvents would enable testing different salt and electrolyte configurations for the Ca-mediated NH_3 synthesis, leading to an optimal configuration to maximize NH_3 FE. Similarly, such a study would enable lowering the total cell potential of the system and, therefore, the overall energy efficiency of the process. The role of the SEI in determining the NH_3 FE remains poorly understood, and in situ studies to probe the SEI are required. The presented work would enable future studies of the NH_3 synthesis by using Ca and other materials beyond Li as a mediator.

■ ASSOCIATED CONTENT

Supporting Information

The Supporting Information is available free of charge at https://pubs.acs.org/doi/10.1021/acsenergylett.4c01455.

Methods for electrochemical experiments; colorimetric quantification for MgMAS; details of the materials used; methods for all characterizations performed including NMR, XPS, and SEM; calibration graphs and NMR spectra for $^{14}N_2$ and $^{15}N_2$ ammonia calibration; cell potential vs time during chronopotentiometry for varying current densities from −5 mA/cm^2 to −45 mA/cm^2; ^{1}H NMR spectra for isotope-labeled runs at −15 mA/cm^2 for 2 h; NMR spectra for all control experiments including open circuit control experiments for both $^{15}N_2$ and $^{14}N_2$ pre-electrolyte, as well as post-electrolyte, for control experiment with 6 bar Ar and post-NMR spectra after keeping freshly prepared electrolyte open in the fume hood for 2 h; SEM images of bare Ni foam pre-electrolysis and post-electrolysis (PDF)

■ AUTHOR INFORMATION

Corresponding Authors

Aayush R. Singh − *Dow Inc., Midland, Michigan 48686, United States;* Present Address: SandboxAQ, Palo Alto, California, USA; Email: aayush.singh@sandboxquantum.com

Joseph A. Gauthier − *Department of Chemical Engineering, Texas Tech University, Lubbock, Texas 79409, United States;* orcid.org/0000-0001-9542-0988; Email: Joe.Gauthier@ttu.edu

Meenesh R. Singh − *Department of Chemical Engineering, University of Illinois Chicago, Chicago, Illinois 60607, United States;* orcid.org/0000-0002-3638-8866; Email: mrsingh@uic.edu

Authors

Ishita Goyal − *Department of Chemical Engineering, University of Illinois Chicago, Chicago, Illinois 60607, United States*

Nishithan C. Kani − *Department of Chemical Engineering, University of Illinois Chicago, Chicago, Illinois 60607, United States*

Samuel A. Olusegun − *Department of Chemical Engineering, Texas Tech University, Lubbock, Texas 79409, United States*

Sreenivasulu Chinnabattigalla − *Department of Chemistry, University of Illinois Chicago, Chicago, Illinois 60607, United States; Chemical Sciences and Engineering, Argonne National Laboratory, Lemont, Illinois 60439, United States*

Rajan R. Bhawnani − *Department of Chemical Engineering, University of Illinois Chicago, Chicago, Illinois 60607, United States*

Ksenija D. Glusac − *Department of Chemistry, University of Illinois Chicago, Chicago, Illinois 60607, United States; Chemical Sciences and Engineering, Argonne National Laboratory, Lemont, Illinois 60439, United States;* orcid.org/0000-0002-2734-057X

Complete contact information is available at: https://pubs.acs.org/10.1021/acsenergylett.4c01455

Author Contributions

#I.G. and N.C.K. contributed equally. M.R.S. and J.A.G. conceived the ideas and cowrote the manuscript. I.G. and N.C.K. planned and performed all the electrochemical experiments and cowrote the manuscript. S.A.O., A.R.S., and J.A.G. conducted the DFT calculations. S.C. and K.D.G. helped in the NMR analysis of the post-electrolyte samples. R.B. assisted with the characterization of the electrodes. A.R.S. provided additional support and resources.

Notes

The authors declare the following competing financial interest(s): A provisional patent titled Metal nitride mediated ammonia synthesis, UIC 2023-086 has been filed.

■ ACKNOWLEDGMENTS

This material is based on the work performed in the Materials and Systems Engineering Laboratory at the University of Illinois Chicago (UIC) and the Gauthier Laboratory at Texas Tech University, in collaboration with Dr. Aayush R. Singh and Glusac's Lab. This work made use of the EPIC facility of Northwestern University's NUANCE Center, which has received support from the SHyNE Resource (NSF ECCS-2025633), the IIN, and Northwestern's MRSEC program

https://doi.org/10.1021/acsenergylett.4c01455
ACS Energy Lett. 2024, 9, 4188−4195

(NSF DMR-1720139). This work also made use of the Keck-II facility of Northwestern University's NUANCE Center, which has received support from the SHyNE Resource (NSF ECCS-2025633), the IIN, and Northwestern's MRSEC program (NSF DMR-2308691). This work made use of the IMSERC at Northwestern University, which has received support from the NSF (CHE-1048773 and DMR0521267). K.D.G. acknowledges NSF (CHE-2102247) for financial support. S.A.O. and J.A.G. gratefully acknowledge support from The Welch Foundation under Grant Number D-2188-20240404.

REFERENCES

(1) MacFarlane, D. R.; Cherepanov, P. V.; Choi, J.; Suryanto, B. H.; Hodgetts, R. Y.; Bakker, J. M.; Vallana, F. M. F.; Simonov, A. N. A roadmap to the ammonia economy. *Joule* **2020**, *4* (6), 1186−1205.

(2) Erisman, J. W.; Sutton, M. A.; Galloway, J.; Klimont, Z.; Winiwarter, W. How a century of ammonia synthesis changed the world. *Nature geoscience* **2008**, *1* (10), 636−639.

(3) Christensen, C. H.; Johannessen, T.; Sørensen, R. Z.; Nørskov, J. K. Towards an ammonia-mediated hydrogen economy? *Catal. Today* **2006**, *111* (1−2), 140−144.

(4) Shipman, M. A.; Symes, M. D. Recent progress towards the electrosynthesis of ammonia from sustainable resources. *Catal. Today* **2017**, *286*, 57−68.

(5) Fu, X.; Zhang, J.; Kang, Y. Recent advances and challenges of electrochemical ammonia synthesis. *Chem. Catalysis* **2022**, *2* (10), 2590−2613.

(6) Qing, G.; Ghazfar, R.; Jackowski, S. T.; Habibzadeh, F.; Ashtiani, M. M.; Chen, C.-P.; Smith, M. R., III; Hamann, T. W. Recent Advances and Challenges of Electrocatalytic N2 Reduction to Ammonia. *Chem. Rev.* **2020**, *120* (12), 5437−5516.

(7) Du, H.-L.; Chatti, M.; Hodgetts, R. Y.; Cherepanov, P. V.; Nguyen, C. K.; Matuszek, K.; MacFarlane, D. R.; Simonov, A. N. Electroreduction of nitrogen with almost 100% current-to-ammonia efficiency. *Nature* **2022**, *609* (7928), 722−727.

(8) Choi, J.; Du, H.-L.; Nguyen, C. K.; Suryanto, B. H.; Simonov, A. N.; MacFarlane, D. R. Electroreduction of nitrates, nitrites, and gaseous nitrogen oxides: a potential source of ammonia in dinitrogen reduction studies. *ACS Energy Lett.* **2020**, *5* (6), 2095−2097.

(9) Andersen, S. Z.; Čolić, V.; Yang, S.; Schwalbe, J. A.; Nielander, A. C.; McEnaney, J. M.; Enemark-Rasmussen, K.; Baker, J. G.; Singh, A. R.; Rohr, B. A. A rigorous electrochemical ammonia synthesis protocol with quantitative isotope measurements. *Nature* **2019**, *570* (7762), 504−508.

(10) Andersen, S. Z.; Statt, M. J.; Bukas, V. J.; Shapel, S. G.; Pedersen, J. B.; Krempl, K.; Saccoccio, M.; Chakraborty, D.; Kibsgaard, J.; Vesborg, P. C. Increasing stability, efficiency, and fundamental understanding of lithium-mediated electrochemical nitrogen reduction. *Energy Environ. Sci.* **2020**, *13* (11), 4291−4300.

(11) Kani, N. C.; Goyal, I.; Gauthier, J. A.; Shields, W.; Shields, M.; Singh, M. R. Pathway toward Scalable Energy-Efficient Li-Mediated Ammonia Synthesis. *ACS Appl. Mater. Interfaces* **2024**, *16* (13), 16203−16212.

(12) Sažinas, R.; Li, K.; Andersen, S. Z.; Saccoccio, M.; Li, S.; Pedersen, J. B.; Kibsgaard, J.; Vesborg, P. C.; Chakraborty, D.; Chorkendorff, I. Oxygen-Enhanced Chemical Stability of Lithium-Mediated Electrochemical Ammonia Synthesis. *J. Phys. Chem. Lett.* **2022**, *13* (20), 4605−4611.

(13) Lazouski, N.; Schiffer, Z. J.; Williams, K.; Manthiram, K. Understanding continuous lithium-mediated electrochemical nitrogen reduction. *Joule* **2019**, *3* (4), 1127−1139.

(14) Lazouski, N.; Steinberg, K. J.; Gala, M. L.; Krishnamurthy, D.; Viswanathan, V.; Manthiram, K. Proton donors induce a differential transport effect for selectivity toward ammonia in lithium-mediated nitrogen reduction. *ACS Catal.* **2022**, *12* (9), 5197−5208.

(15) Lazouski, N.; Chung, M.; Williams, K.; Gala, M. L.; Manthiram, K. Non-aqueous gas diffusion electrodes for rapid ammonia synthesis from nitrogen and water-splitting-derived hydrogen. *Nature Catalysis* **2020**, *3* (5), 463−469.

(16) Sažinas, R.; Andersen, S. Z.; Li, K.; Saccoccio, M.; Krempl, K.; Pedersen, J. B.; Kibsgaard, J.; Vesborg, P. C. K.; Chakraborty, D.; Chorkendorff, I. Towards understanding of electrolyte degradation in lithium-mediated non-aqueous electrochemical ammonia synthesis with gas chromatography-mass spectrometry. *RSC Adv.* **2021**, *11* (50), 31487−31498.

(17) Li, K.; Shapel, S. G.; Hochfilzer, D.; Pedersen, J. B.; Krempl, K.; Andersen, S. Z.; Sažinas, R.; Saccoccio, M.; Li, S.; Chakraborty, D. Increasing Current Density of Li-Mediated Ammonia Synthesis with High Surface Area Copper Electrodes. *ACS Energy Lett.* **2022**, *7* (1), 36−41.

(18) Li, K.; Andersen, S. Z.; Statt, M. J.; Saccoccio, M.; Bukas, V. J.; Krempl, K.; Sažinas, R.; Pedersen, J. B.; Shadravan, V.; Zhou, Y. Enhancement of lithium-mediated ammonia synthesis by addition of oxygen. *Science* **2021**, *374* (6575), 1593−1597.

(19) Li, S.; Zhou, Y.; Li, K.; Saccoccio, M.; Sažinas, R.; Andersen, S. Z.; Pedersen, J. B.; Fu, X.; Shadravan, V.; Chakraborty, D. Electrosynthesis of ammonia with high selectivity and high rates via engineering of the solid-electrolyte interphase. *Joule* **2022**, *6* (9), 2083−2101.

(20) Fu, X.; Pedersen, J. B.; Zhou, Y.; Saccoccio, M.; Li, S.; Sažinas, R.; Li, K.; Andersen, S. Z.; Xu, A.; Deissler, N. H. Continuous-flow electrosynthesis of ammonia by nitrogen reduction and hydrogen oxidation. *Science* **2023**, *379* (6633), 707−712.

(21) Cherepanov, P. V.; Krebsz, M.; Hodgetts, R. Y.; Simonov, A. N.; MacFarlane, D. R. Understanding the factors determining the faradaic efficiency and rate of the lithium redox-mediated N2 reduction to ammonia. *J. Phys. Chem. C* **2021**, *125* (21), 11402−11410.

(22) Rakov, D.; Hasanpoor, M.; Baskin, A.; Lawson, J. W.; Chen, F.; Cherepanov, P. V.; Simonov, A. N.; Howlett, P. C.; Forsyth, M. Stable and Efficient Lithium Metal Anode Cycling through Understanding the Effects of Electrolyte Composition and Electrode Preconditioning. *Chem. Mater.* **2022**, *34* (1), 165−177.

(23) Suryanto, B. H.; Matuszek, K.; Choi, J.; Hodgetts, R. Y.; Du, H.-L.; Bakker, J. M.; Kang, C. S.; Cherepanov, P. V.; Simonov, A. N.; MacFarlane, D. R. Nitrogen reduction to ammonia at high efficiency and rates based on a phosphonium proton shuttle. *Science* **2021**, *372* (6547), 1187−1191.

(24) Blair, S. J.; Doucet, M.; Niemann, V. A.; Stone, K. H.; Kreider, M. E.; Browning, J. F.; Halbert, C. E.; Wang, H.; Benedek, P.; McShane, E. J.; et al. Combined, time-resolved, in situ neutron reflectometry and X-ray diffraction analysis of dynamic SEI formation during electrochemical N2 reduction. *Energy Environ. Sci.* **2023**, *16* (8), 3391−3406.

(25) Montoya, J. H.; Tsai, C.; Vojvodic, A.; Nørskov, J. K. The Challenge of Electrochemical Ammonia Synthesis: A New Perspective on the Role of Nitrogen Scaling Relations. *ChemSusChem* **2015**, *8* (13), 2180−2186.

(26) Tort, R.; Bagger, A.; Westhead, O.; Kondo, Y.; Khobnya, A.; Winiwarter, A.; Davies, B. J. V.; Walsh, A.; Katayama, Y.; Yamada, Y.; et al. Searching for the Rules of Electrochemical Nitrogen Fixation. *ACS Catal.* **2023**, *13* (22), 14513−14522.

(27) Singh, A. R. *A Theoretical Approach Toward Sustainable Ammonia Synthesis*. Ph.D. Dissertation, Stanford University, 2019.

(28) Choksi, T. S.; Roling, L. T.; Streibel, V.; Abild-Pedersen, F. Predicting adsorption properties of catalytic descriptors on bimetallic nanoalloys with site-specific precision. *journal of Physical Chemistry Letters* **2019**, *10* (8), 1852−1859.

(29) Roling, L. T.; Choksi, T. S.; Abild-Pedersen, F. A coordination-based model for transition metal alloy nanoparticles. *Nanoscale* **2019**, *11* (10), 4438−4452.

(30) Roling, L. T.; Abild-Pedersen, F. Structure-Sensitive Scaling Relations: Adsorption Energies from Surface Site Stability. *ChemCatChem.* **2018**, *10* (7), 1643−1650.

https://doi.org/10.1021/acsenergylett.4c01455
ACS Energy Lett. 2024, 9, 4188−4195

(31) Goyal, I.; Kani, N. Calcium as a Mediator for the Electrochemical Synthesis of NH3. *ChemRxiv* **2023**, DOI: 10.26434/chemrxiv-2023-zchlg.
(32) Fu, X.; Niemann, V. A.; Zhou, Y.; Li, S.; Zhang, K.; Pedersen, J. B.; Saccoccio, M.; Andersen, S. Z.; Enemark-Rasmussen, K.; Benedek, P.; et al. Calcium-mediated nitrogen reduction for electrochemical ammonia synthesis. *Nat. Mater.* **2024**, *23* (1), 101−107.
(33) Schwalbe, J. A.; Statt, M. J.; Chosy, C.; Singh, A. R.; Rohr, B. A.; Nielander, A. C.; Andersen, S. Z.; McEnaney, J. M.; Baker, J. G.; Jaramillo, T. F.; et al. A Combined Theory-Experiment Analysis of the Surface Species in Lithium-Mediated NH3 Electrosynthesis. *ChemElectroChem.* **2020**, *7* (7), 1542−1549.
(34) Medford, A. J.; Vojvodic, A.; Hummelshøj, J. S.; Voss, J.; Abild-Pedersen, F.; Studt, F.; Bligaard, T.; Nilsson, A.; Nørskov, J. K. From the Sabatier principle to a predictive theory of transition-metal heterogeneous catalysis. *J. Catal.* **2015**, *328*, 36−42.
(35) Zhu, S.; Peng, F.; Liu, H.; Majumdar, A.; Gao, T.; Yao, Y. Stable Calcium Nitrides at Ambient and High Pressures. *Inorg. Chem.* **2016**, *55* (15), 7550−7555.
(36) Ehrlich, P. Calcium, Strontium, Barium Nitride Ca3N2, Sr3N2, Ba3N2. In *Handbook of Preparative Inorganic Chemistry*, 2nd ed.; 1963; Vol. *1*, p 940−941.

https://doi.org/10.1021/acsenergylett.4c01455
ACS Energy Lett. 2024, 9, 4188−4195